Talanta 219 (2020) 121216

Contents lists available at ScienceDirect

Talanta

journal homepage: www.elsevier.com/locate/talanta

Development of non-equilibrium rapid replacement aptamer assay for ultra-fast detection of phthalic acid esters

Dabin Kim[a], Hyun Jeong Lim[a], Yun Gyong Ahn[b], Beelee Chua[c,*], Ahjeong Son[a,**]

[a] Department of Environmental Science and Engineering, Ewha Womans University, Seoul, 03760, Republic of Korea
[b] Western Seoul Center, Korea Basic Science Institute, Seoul, 03760, Republic of Korea
[c] School of Electrical Engineering, Korea University, Seoul, 02841, Republic of Korea

ARTICLE INFO

Keywords:
Phthalic acid esters (PAEs)
Endocrine disrupting chemicals
Aptamer
Biosensor
Ultra-fast detection
Portable device

ABSTRACT

In this paper, we developed a non-equilibrium rapid replacement aptamer (NERRA) assay that performed ultra-fast (in 30 s) quantitative detection of phthalic acid esters (PAEs) without waiting for the reaction to reach equilibrium. NERRA assay employed fluorescence PoPo3 dye intercalated in an ssDNA aptamer to selectively detect and quantify the PAEs in water. As the intercalated dye was replaced by the PAEs and quenched in the water, the rate of fluorescence change became proportional to PAEs concentration. The sensitivity of NERRA assay was first evaluated with a commercial spectrofluorometer. The selectivity for PAE mixture, individual PAEs, and non-phthalate compounds were also investigated. NERRA assay was also able to quantitatively detect the PAEs in a common plastic product (picnic mat), and the results were compared with those of gas chromatography mass spectrometry. Finally, a custom analyzer (8.5 cm × 8.5 cm × 16.5 cm) was built to demonstrate the portability of the NERRA assay. Using a commercial spectrofluorometer, NERRA assay was able to quantitatively detect a PAE mixture in 30 min with an LOQ of 0.1 μg/L. Using the portable custom analyzer, the detection time was shortened to 30 s with a tradeoff in the LOQ (1 μg/L). In both cases, the LOQs remain within the environmentally relevant PAE concentrations of 0.1–1472 μg/L.

1. Introduction

In the early 1900s, the first fully synthetic material (Bakelite) was created; it became the basis of the entire emerging family of new materials that is, today, collectively known as plastics. Plastic, in a literal sense, means moldable in Greek (*plastikos*). The ubiquity of plastics in every aspect of our lives is attributable to their versatility of assuming complex shapes and the accompanying durability.

However, a more sinister aspect of this miracle material began to surface in the second half of the 1900s. The legendary mechanical properties of plastics, such as polyvinyl chloride (PVC), are only possible because of the addition of plasticizers, such as phthalic acid esters (PAEs) or phthalates [1–4]. In fact, plasticizers are so important that their loss is the dominant cause of mechanical degradation in PVC pipes [4]. The loss of plasticizers could be via migration, volatilization, or leaching into surrounding media, such as water [5,6]. These loss mechanisms could also apply to other plasticizer-filled consumer plastic products, such as food packaging and children toys [7–12]. More specifically, a percentage of the approximate 8 million tons of plasticizers produced globally every year will eventually be “lost” and find their way into our environment, particularly into water.

Plasticizers such as PAEs possess an insidious nature due to their molecular similarity to human hormones. Once ingested, they behave like human hormones and disrupt the endocrine system [13]. The notoriety that they have gained by interfering with reproduction and metabolism overshadows their carcinogenicity [14–16]. If PAEs enter water and soils, they can move up the food chain and eventually into the human body. Among the PAEs, di-2-ethylhexyl phthalate (DEHP) has often been selected for regulation owing to its widespread use [17]. In fact, it has already been regulated (no more than 6 μg/L in drinking water) by the United States Environmental Protection Agency [18]. However, the problem is not limited to DEHP. It is proven that the different analogs of DEHP such as DBP, DIBP, BBP, DNHP, DNPP, DCHP, and DIBP (abbreviations are listed in SI), are no less insidious with regard to their effects on human health [19–22]; hence, they are also regulated [18,23].

Currently, the quantitative detection of PAEs in environmental samples are mostly undertaken by conventional laboratory-based

* Corresponding author. 145 Anam-ro, Seongbuk-gu, Korea University, Seoul, 02841, Republic of Korea.
** Corresponding author. 52 Ewhayeodae-gil, Seodaemun-gu, Ewha Womans University, Seoul, 03760, Republic of Korea.
E-mail addresses: bchua@korea.ac.kr, chuabeelee@gmail.com (B. Chua), ason@ewha.ac.kr, ahjeong.son@gmail.com (A. Son).

https://doi.org/10.1016/j.talanta.2020.121216
Received 12 March 2020; Received in revised form 21 May 2020; Accepted 22 May 2020
Available online 02 June 2020

Table 1
Detection time, assay selectivity, assay sensitivity, and portability of various biosensor technologies for phthalate detection.

Biosensor Technology		Target Phthalates	Detection Time	Assay Selectivity	Assay Sensitivity (LOQ and range of quantification, μg/L)	Portability	References
Grouped phthalates	NERRA assay	7 Phthalic acid esters[a]	30 s–30 min[b]	● Non-phthalate chemicals (BPA and 4-NP) (Signals of BPA and 4-NP are ~77% signal of PAEs)	0.1–200 as PAEs	Yes	This study
	Immunoassay	8 Phthalic acid esters[c]	~ 0.67 h	● No selectivity tested	0.01–100 as PAEs	No	[28]
Individual phthalate	Immunoassay	DEHP	~ 6 h	● DMP, DEP, DPrP, DBP, DAP, DCHP, and 4-DEHAP (Cross-reactivity: < 0.01%–57%)	0.001–1000 as DEHP	No	[29]
		DIBP	~ 18 h	● DCHP, DiBAP, DNOP, DMP, DEP, and DBP (Cross-reactivity: < 0.61%–12.07%)	10–357 as DiBP	No	[30]
		DBP	~ 17 h	● DMP, DEP, DPrP, DPP, DEHP, DCHP, DBNP, and DBAP (Cross-reactivity: 0.9%–22.7%)	0.1–100 as DBP	No	[31]
		DBP	~ 21 h	● DOP, DNHP, DMP, DBEP, DEEP, DPP, BBP, DCHP, DIBP, DEHP, 4-NPA, and DBaP (Cross-reactivity: < 1%–4.8%)	5–250 as DBP	No	[32,33]
	Aptasensor	DEHP	~ 3 h	● Phthalic acid and other non-phthalate chemicals (~10% signal reduction for phthalic acid and other chemicals compared to ~40% signal reduction for DEHP)	0.0039–39 as DEHP	No	[34]
		DEHP	~ 6 h	● DMP, DEP, DBP, DHP, DIBP, DINP, BBP, and DPP (0%–25% signal reduction for all 8 other phthalates compared to ~38% for DEHP)	0.0005–100 as DEHP	Yes	[35]
	Other sensors	DBP	~ 0.5 h	● MIP sensor for DEP, DMP, and DAP (Signals of DEP, DMP, and DAP are 50%–75% signal of DBP)	1391–13,917 as DBP	No	[36]
		DEHP	~ 2 h	● Impedance values of non-phthalate chemicals were tested	781–7030 as DEHP	No	[37]

Notes).
[a] Indicates 7 phthalate chemicals comprising PA, DMP, DEP, DBP, DIBP, BBP, and DEHP.
[b] Indicates the detection time performed by both the portable analyzer (30 s) and laboratory assay (30 min).
[c] Indicates 8 phthalate chemicals comprising DMP, DEP, DBP, BBP, DEHP, DCHP, DnOP, and DNP.

analytical techniques, such as gas chromatography-mass spectrometry, high-performance liquid chromatography, or liquid chromatography-tandem mass spectrometry [24–27]. These methods are accurate and precise, but also time-consuming and require large-footprint equipment. Alternative quantitative detection methods include immunoassays [28–33], aptasensors [34,35], and other types of sensors, such as a molecularly imprinted polymer sensor [36,37]. The quantitative detection time of these alternative methods are at least 30 min, and up to 21 h (Table 1). Given the scale of contamination and the accompanying large number of environmental samples that require analysis, the quantitative detection time clearly requires improvement. However, the existing methods are unable to surpass the current paradigm because they are bounded by the axiom that sensing can only be performed at equilibrium, which can only be achieved after a significant duration.

In this study, we overturned the abovementioned axiom and demonstrated a non-equilibrium rapid replacement aptamer (NERRA) assay that would allow ultra-fast quantitative detection with both a commercial spectrofluorometer and a custom-built analyzer. The building blocks of NERRA assay are based on well-known label-free fluorescence assays [38–41]. Furthermore, NERRA assay comprises a target-specific ssDNA aptamer intercalated with a water-quenchable fluorescence dye. Unlike FRET sensors, the proposed assay does not require an additional fluorescence donor or acceptor [42–44]. Instead, the intercalated fluorescence dye is directly excited by a laser or LED source. As shown in Fig. 1a, in the presence of a target, the intercalated fluorescence dye is rapidly replaced and quenched in the water. This reduces the emitted fluorescence (561 nm). Unlike conventional methods, NERRA assay could detect and quantify the target without waiting for the reaction (hence, fluorescence) to reach equilibrium.

Using the aptamer previously designed by Han et al., for PAEs [34], PoPo3 as an intercalating fluorescence dye and a commercial spectrofluorometer, we first established the appropriate ratio of ssDNA aptamer to PoPo3. Using varying concentrations of PAEs (PA, DMP, DEP, DBP, DIBP, BBP, and DEHP), we demonstrated the feasibility of NERRA assay. As shown in Fig. 1b, the target concentration was deduced from the rate of fluorescence change $|\Delta RFU_{561}/\Delta t|$ instead of the normalized fluorescence ($RFU_{561\ nm}$-$RFU_{reference}/RFU_{reference}$). For example, a higher target concentration would result in a higher value of $|\Delta RFU_{561}/\Delta t|$. Using the same metric $|\Delta RFU_{561}/\Delta t|$, the selectivity of NERRA assay to PAE mixtures, individual PAEs, and non-phthalate compounds were investigated. In addition, we employed NERRA assay to detect and quantify the amount of PAEs in a plastic product (*i.e.*, a picnic mat) for comparison with the gas chromatography mass spectrometry (GC/MS) analysis. A custom analyzer was also built to demonstrate the portability of the NERRA assay and to improve its detection time. As shown in Fig. 1c, the target concentration could be alternatively deduced from the rate of output voltage change ($\Delta V_{out}/\Delta t$).

2. Materials and methods

2.1. Conformational change analysis of ssDNA aptamer binding with PAEs

An ssDNA aptamer (5′-CTT TCT GTC CTT CCG TCA CAT CCC ACG CAT TCT CCA CAT-3′, Bioneer Corp., Daejeon, Korea) [34] was used for the collective detection of seven PAEs. The binding affinity of the aptamer to the PAEs as well as PoPo3 was examined using circular dichroism (CD) spectropolarimetry. A total of 30 μL of 25 μM aptamer was added to 240 μL of 0.02 M Tris-HCl buffer (0.02 M of Tris-base, pH 8.0, Sigma-Aldrich, Saint Louis, MO, USA) containing 0.005% of sodium dodecyl sulfate (SDS, Sigma-Aldrich), 0.02 M of $MgCl_2{\cdot}H_2O$ (Daejung, Gyeonggi, Korea), 0.04 M of KCl (Duksan, Seoul, Korea), and 0.1 M of NaCl (Junsei, Tokyo, Japan). Subsequently, 30 μL of PAEs (1 and 10 μg/L as final concentrations) was added to the solution (a total of 300 μL). Similar experiment was perfomed for PoPo3 (1 and 5 μg/L as final concentrations). The 0.02 M Tris-HCl buffer was used as a

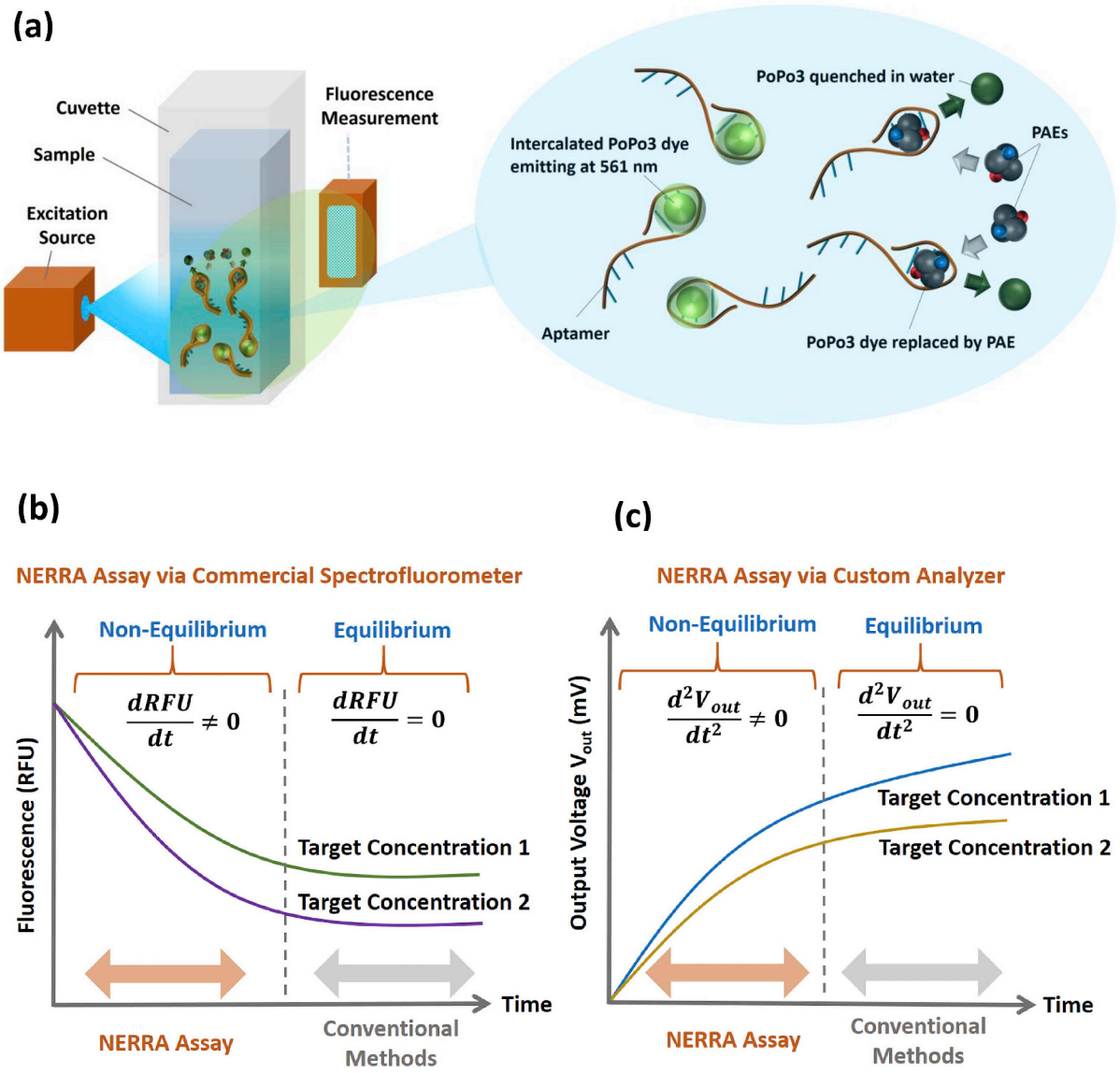

Fig. 1. (a) Schematic of NERRA assay; (b) Operation of NERRA assay via commercial spectrofluorometer; (b) Operation of custom analyzer.

baseline control. Nitrogen purging was performed prior to CD measurement. The CD spectra were obtained from 500 nm to 200 nm at a scan speed of 200 nm/min by a Jasco J1500 spectropolarimeter (Jasco Inc., Easton, MD, USA). The length of the quartz cuvette was 1 mm. In addition, the ellipticity was calculated from three measurements, and the baseline was subtracted from the results.

2.2. Determination of suitable PoPo3 dye and ssDNA aptamer concentrations

Determination of suitable ssDNA aptamer concentration. A total of 20 μL of PoPo3 dye (PoPo™-3 iodide dye, dimeric cyanine nucleic acid stains, Invitrogen, Carlsbad, CA, USA) and 20 μL of ssDNA aptamer were mixed with 160 μL of 0.02 M Tris-HCl buffer in an opaque 96-well microplate (SPL, Gyeonggi, Korea) to achieve the varying final concentrations of the PoPo3 dye (0, 0.1, 1, 5, and 10 μM) and the ssDNA aptamer (0, 0.05, 0.25, 0.5, and 2.5 μM). The total reaction volume was 200 μL, and the solution was incubated for 3 min at ambient temperature without shaking. The fluorescence measurement was performed with a SpectraMax M2 spectrofluorometer (Molecular Devices, Sunnyvale, CA, USA) at emission and excitation wavelengths of 561 nm and 530 nm, respectively.

Determination of suitable PoPo3 dye concentration. Using the procedure described earlier, samples with varying final PoPo3 dye concentrations (0, 0.1, 1, 5, and 10 μM) and an accompanying final ssDNA aptamer concentration of 2.5 μM were prepared. After preparation, the samples were immediately subjected to fluorescence measurement for 10 min at 1 min intervals by the SpectraMax M2 spectrofluorometer.

Comparison with negative controls. Using the procedure described earlier, a sample with a final PoPo3 dye concentration of 1 μM and an accompanying final ssDNA aptamer concentration of 2.5 μM (Aptamer + PoPo3 + Buffer) was prepared. Together with two negative controls (NCs; PoPo3 + Buffer and Buffer only), the sample was subjected to fluorescence measurement for 10 min at 1 min intervals by the SpectraMax M2 spectrofluorometer.

2.3. Characterization of quantification sensitivity of NERRA assay to PAEs

Aliquots comprising 10 μM PoPo3 dye (20 μL) and 25 μM aptamer (20 μL) were transferred into the microplate and mixed with 140 μL of 0.02 M Tris-HCl buffer for intercalation (3 min). After intercalation, 20 μL of the PAE mixture at varying concentrations (0.1, 1, 5, 50, and 200 μg/L as final concentrations) was added to the microplate, resulting

in a total reaction volume of 200 μL. As shown in Table S1, the PAE mixture included phthalic acid (PA), dimethyl phthalate (DMP), diethyl phthalate (DEP), di-n-butyl phthalate (DBP), diisobutyl phthalate (DIBP), benzyl butyl phthalate (BBP), and di-2-ethylhexyl phthalate (DEHP). The PAEs used in the mixture were purchased from AccuStandard (New Haven, CT, USA), except for PA (Sigma-Aldrich). For the NC, ultrapure distilled water (Ultrapure™ DNase/RNase Free Distilled Water, Invitrogen) was added instead of the PAE mixture. Immediately after the addition of the PAE mixture (or NC), the fluorescence measurement was performed for 30 min at 2 min intervals by the SpectraMax M2 spectrofluorometer. The rate of fluorescence change $|\Delta RFU_{561}/\Delta t|$ is calculated as follows:

$$\text{Rate of fluorescence change} \left(\left| \frac{\Delta RFU_{561\ nm}}{\Delta t} \right| \right) = \left| \frac{RFU_{final} - RFU_{initial}}{t_{final} - t_{initial}} \right| \quad (1)$$

where $t_{initial}$ and t_{final} are the start and stop times of the fluorescence measurement, and $RFU_{initial}$ and RFU_{final} are the corresponding fluorescence values at these time points.

It is important to mention that the fluorescence measurement at a single time point usually yields a significant result once the reaction has achieved equilibrium. However, to yield a meaningful result during non-equilibrium, a cumulative representation over a time interval will be essential. In this regard, the rate of fluorescence change $|\Delta RFU_{561}/\Delta t|$ will be a suitable cumulative representation.

2.4. Characterization of quantification selectivity of NERRA assay to PAEs

The selectivity of NERRA assay to a PAE mixture, individual PAEs (PA, DMP, DEP, DBP, DIBP, BBP, and DEHP), as well as non-phthalate compounds (bisphenol A and 4-nonyl phenol) was characterized. Detailed information on the non-phthalate compounds is listed in Table S2. Ultrapure distilled water was also used as an NC. Aliquots comprising 10 μM PoPo3 dye (20 μL) and 25 μM ssDNA aptamer (20 μL) were transferred into the microplate and mixed with 140 μL of 0.02 M Tris-HCl buffer for intercalation (3 min). Twenty μL of the target (PAE mixture, individual PAEs, or non-phthalate compounds, 100 μg/L) was added. The total reaction volume was 200 μL. The fluorescence measurements and rate of fluorescence change calculation were performed as previously described.

2.5. Quantitative detection of PAEs in a plastic product

Extraction of organic phase. A commercially available picnic mat was selected as the plastic product to be analyzed by NERRA assay. To extract the organic phase from the plastic product, a portion (300 mg) was incubated in 30 mL of methanol (HPLC grade, JT Baker, Philipsburg, NJ, USA) overnight in a shaking incubator (80 rpm, WIS-30R, Daihan Scientific Corp., Gangwondo, Korea) at ambient temperature. The extracted organic phase would be subjected to both NERRA assay and GC/MS analysis. As NERRA assay is a water-based assay, and to ensure the solubility of the PAEs in water for the NERRA assay, the organic phase was further diluted (1000×) with ultrapure distilled water. This dilution was verified subsequently to be appropriate because the PAE (predominantly DEHP) concentration was 0.16 ± 0.05 mg/L, which is within its solubility in water (0.29 mg/L, Table S1).

Quantitative detection by NERRA assay. Twenty μL of the diluted sample was transferred to 180 μL of Tris-HCl buffer and intercalated PoPo3-aptamer complex. The subsequent fluorescence measurement was performed by the SpectraMax M2 spectrofluorometer. The rate of fluorescence change ($\Delta RFU_{561}/\Delta t$) was calculated using Eq. (1). The corresponding concentration of PAEs (mg/L) was obtained from Fig. 4b, and was further converted from mg/L to mg/kg of sample.

Quantitative detection by GC/MS. The DEHP standard solution was purchased from AccuStandard and dissolved in methanol to achieve a final concentration of 10,000 mg/L. Varying concentrations of the DEHP standard solution (0, 1, 5, 10, 50, 100, 200, 500, and 1000 mg/L in methanol) were prepared by serial dilution with methanol to construct a DEHP calibration curve. As shown in Fig. S1, the contents of the extracted organic phase were identified as mostly DEHP. GC/MS (7820A-5977E, Agilent Technologies, Santa Clara, CA, USA) was operated in both the scan and SIM modes. The m/z ratio for DEHP quantification was set to 149 and 167. A DB-5MS column (Agilent) with a length of 30 m, diameter of 250 μm, and film thickness of 0.25 μm was used. In addition, helium gas was used as the carrier gas at a pressure of 7.23 psi. Splitless injection was used with an injection volume set to 1 μL. Meanwhile, the inlet temperature was set to 280 °C and the oven temperature was changed as follows: initial temperature was set at 50 °C for 1.5 min, then increased to 320 °C at a rate of 15 °C/min, where it was maintained for 4.5 min [45]. The peak area of DEHP corresponding to the extracted organic phase was converted to DEHP concentration (mg/L) using the DEHP calibration curve (Fig. S2). The unit was subsequently converted from mg/L to mg/kg sample.

2.6. Design and operation of custom analyzer

To demonstrate the portability of NERRA assay, a custom analyzer was constructed. As shown in Fig. 2a, the custom analyzer comprised an analysis enclosure and an electronic enclosure. A cuvette holder was placed inside the analysis enclosure to minimize external perturbation during measurement. An LED (10 W, wavelength centered at 400–405 nm, Epiled, China) was positioned on one side of the cuvette holder. Photodiodes (S6429-01, centered at 540 nm, Hamamatsu Photonics, Japan) were also positioned on the sides of the cuvette holder and were orthogonal to the LED. The switching of the LED was controlled by a microcontroller board (OrangeBoard, Kocoafab, Korea). A heatsink and fan (Model MF15B-05, SEPA Europe GmbH, Eschbach, Germany) were used to cool the LED during operation. The auxiliary components included a 16 × 2 LCD (Hitachi HD44780 equivalent with PCF8574AT based I2C backpack module) and a 4 × 4 matrix keypad. The LED voltage was controlled separately via a potentiometer. The output from the photodiodes were directed to a charge integrator, similar to that employed by Lim et al. [35], comprising a low-cost operational amplifier (LTC1051, Linear Technologies, USA) as well as a 10 μF feedback capacitor. The output voltage from the charge integrator was monitored by both the microcontroller board, as well as an external datalogger (Volt101A, MadgeTech Inc, NH, USA) and a computer. The external datalogger was employed because the custom analyzer is yet to be fitted with a built-in datalogger. The top views of the electronics enclosure and analysis enclosure are shown in Fig. 2b and c, respectively, with overall dimensions of 8.5 cm × 8.5 cm × 16.5 cm. The analysis enclosure was positioned on top of the electronics enclosure (Fig. 2d) as this ensured the ease of loading and unloading of the sample-laden cuvette into the cuvette holder.

Prior to operation, the LED voltage was set via the potentiometer. The measurement duration was also programmed via the keypad. The sample-laden cuvette was placed into the cuvette holder and covered with an opaque lid to minimize noise from ambient light. When the start button was pressed, the sample-laden cuvette would be illuminated by the LED. Although the LED was centered at ~410 nm, its spectrum extended to 530 nm (which was necessary to excite the PoPo3 dye). As the PoPo3 dye was gradually replaced by the PAEs and quenched, the fluorescence emission at 561 nm also gradually decreased until it eventually reached equilibrium. This gradual decrease in the fluorescence translated into a decreasing photodiode current. The relationship between the decreasing fluorescence, photodiode current, and the charge integrator output voltage could be described as follows:

$$\frac{dRFU_{561\ nm}}{dt} \propto \frac{dI}{dt} \quad (2a)$$

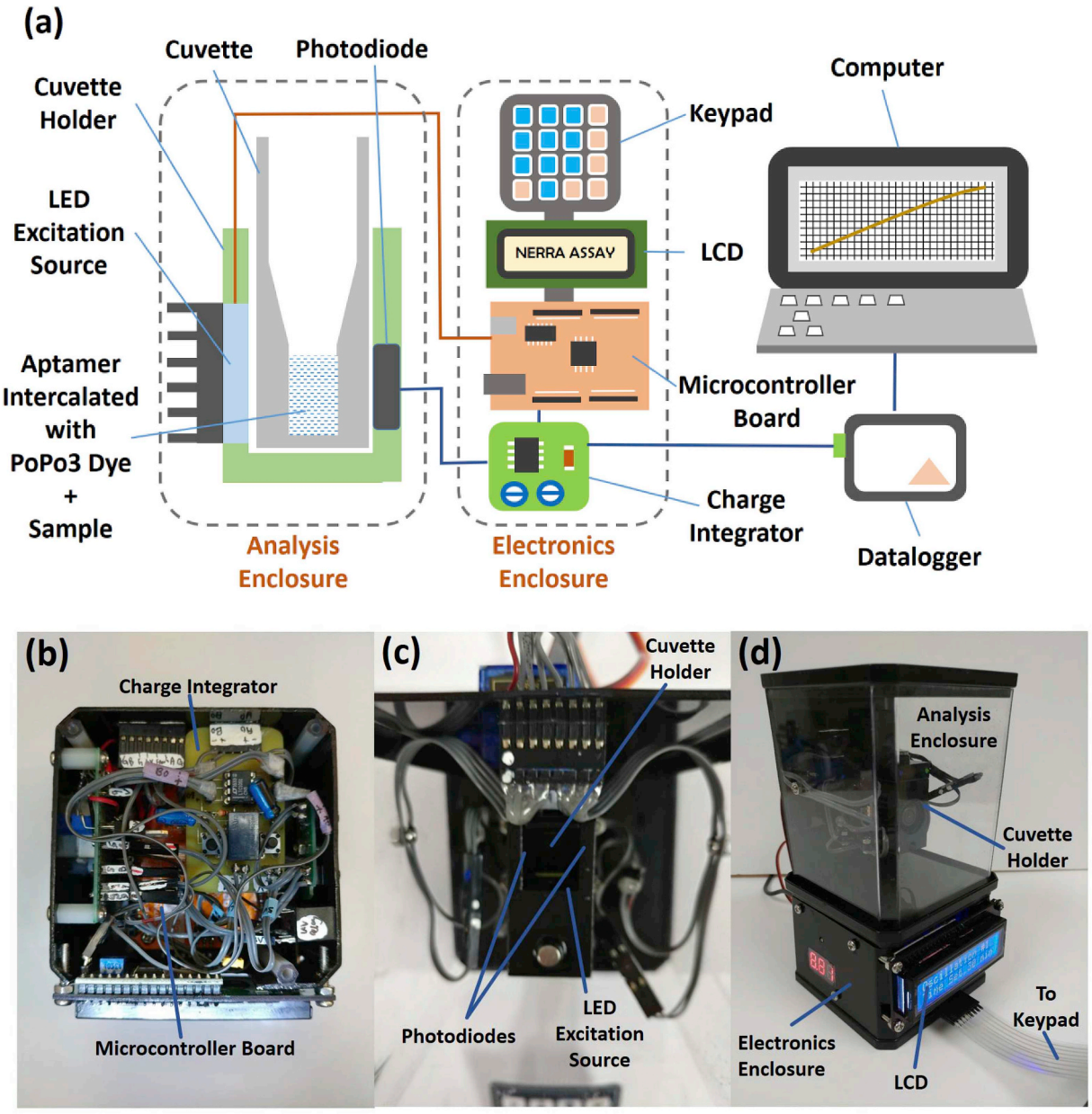

Fig. 2. (a) Schematic of custom analyzer; Photos of custom analyzer: (b) Top view of electronics enclosure; (c) Top view of analysis enclosure; (d) Assembled view.

$$\frac{dI}{dt} = C\frac{d^2V_{out}}{dt^2} \tag{2b}$$

where $RFU_{561\ nm}$ is the fluorescence, I is the photodiode current, C is the capacitor in the charge integrator, V_{out} is the charge integrator output voltage, and t is time. For a given time interval Δt, we could further simplify the relationships in Eqs. (2a) and (2b) as follows:

$$\frac{\Delta RFU_{561\ nm}}{\Delta t} \propto \frac{\Delta I}{\Delta t} \tag{3a}$$

$$\frac{\Delta I}{\Delta t} \propto \frac{\Delta V_{out}}{\Delta t} \tag{3b}$$

The rate of the output voltage change would be proportional to the rate of fluorescence change and the corresponding concentration of PAEs. Similar to the rate of fluorescence change $|\Delta RFU_{561}/\Delta t|$, the rate of the output voltage change ($\Delta V_{out}/\Delta t$) will be an appropriate cumulative representation to yield a significant result for non-equilibrium measurement.

2.7. Quantitative detection of PAEs by custom analyzer

Thirty μL of 10 μM PoPo3 dye and 30 μL of 25 μM ssDNA aptamer were transferred into a cuvette (Q-Vettes semi-micro, Ratiolab®, Hessen, Germany) and mixed with 210 μL of 0.02 M Tris-HCl buffer. After 3 min of intercalation, 30 μL of the PAE mixture at varying concentrations (0, 1, 10, 50, and 100 μg/L) was added to the cuvette (total volume of 300 μL). The cuvette was placed in the cuvette holder of the custom analyzer and covered with an opaque lid. Subsequently, the analyzer was set to excite PoPo3 dye and measure the fluorescence for 5 min. The voltage of the LED excitation source was set to ~8.6 V throughout the measurement. The output voltage V_{out} of the charge integrator was recorded by the datalogger at 1 s intervals. The measurements were performed three times. The rate of output voltage was calculated as shown in Eq. (4).

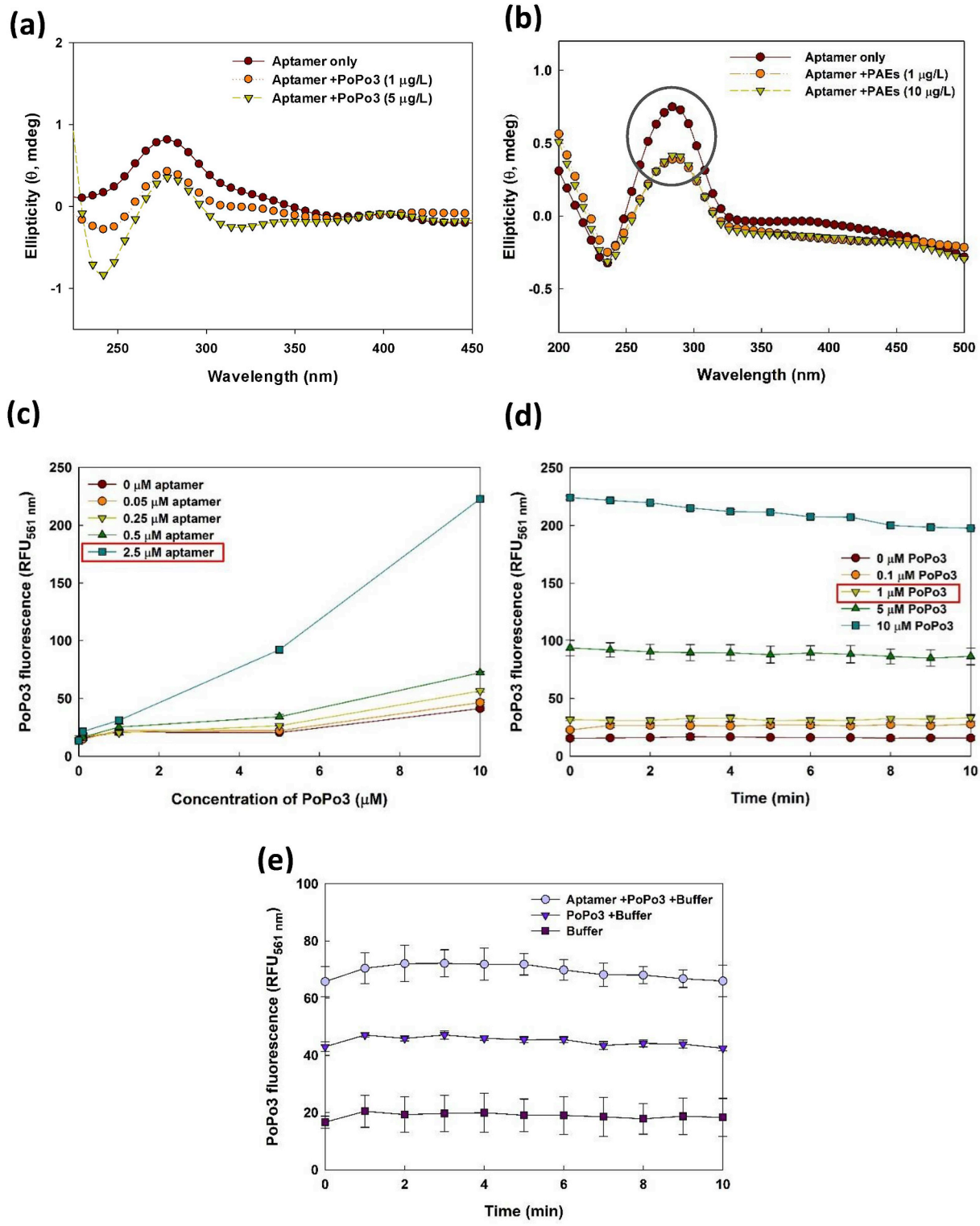

Fig. 3. (a) Circular dichroism (CD) spectral changes of aptamer as a result of PoPo3 intercalation. (b) Circular dichroism (CD) spectral changes of ssDNA aptamer specific to PAE mixture. Determination of suitable (c) ssDNA aptamer and (d) PoPo3 dye concentrations. (e) Comparison with negative controls (NCs). The symbols and error bars indicate the mean and standard deviations of the three measurements; this is the same for Figs. 3–5.

$$\text{Rate of output voltage change } \frac{\Delta V_{out}}{\Delta t}\left(\frac{\text{mV}}{\text{min}}\right) = \frac{V_{final} - V_{initial}}{t_{final} - t_{initial}} \quad (4)$$

where $t_{initial}$ and t_{final} are the start and stop times of measurement, and $V_{initial}$ and V_{final} are the corresponding output voltages V_{out} at these times.

3. Results and discussion

3.1. Conformational change analysis of ssDNA aptamer binding with PAEs

As shown in Fig. 3a, a CD spectral change at ~245 nm was observed as a result of PoPo3 dye intercalation into the aptamer. The negative CD

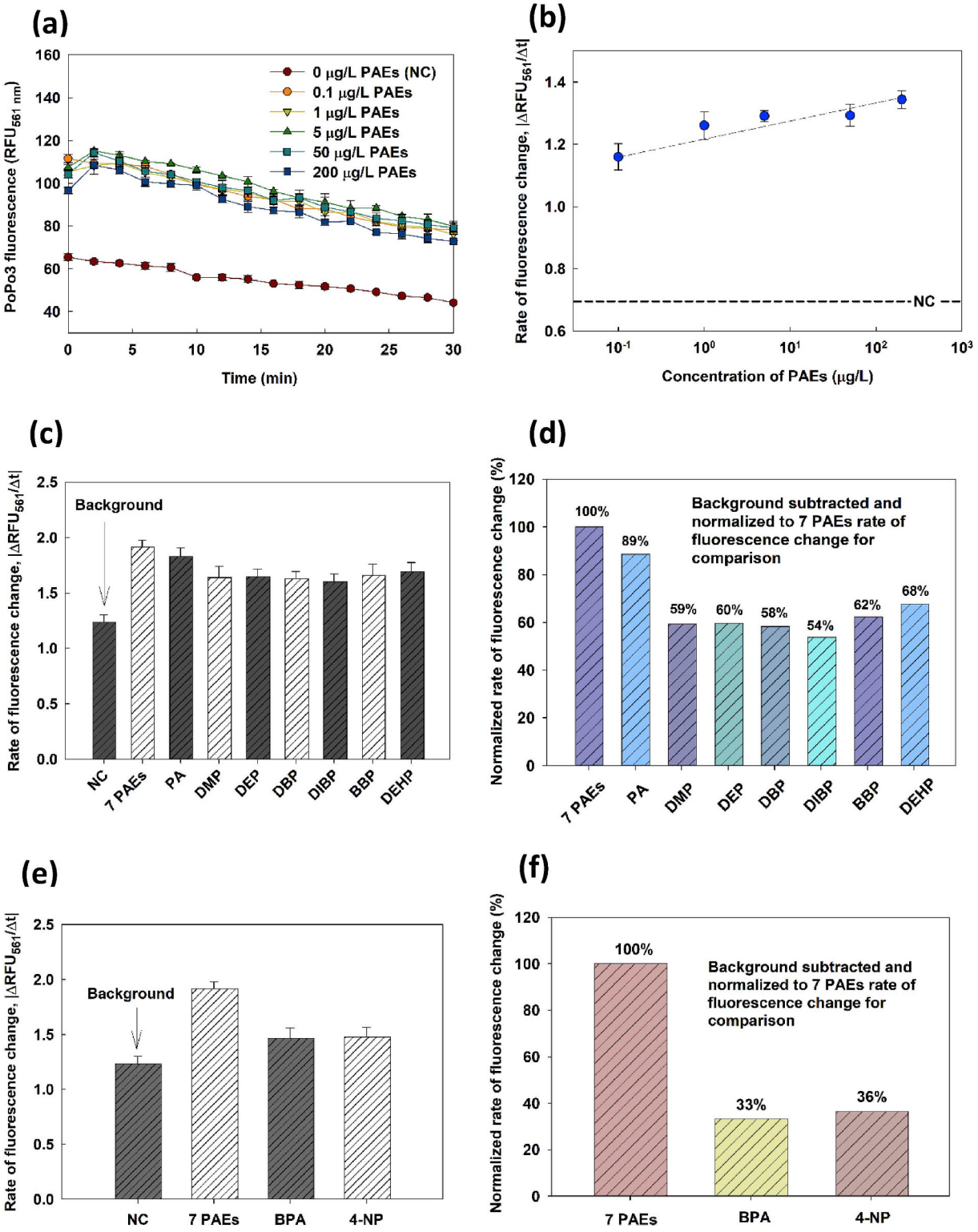

Fig. 4. (a, b) Sensitivity of NERRA assay for PAE quantification: (a) Replacement of PoPo3 dye over time by PAEs; (b) Rate of fluorescence change $|\Delta RFU_{561\ nm}/\Delta t|$ versus concentration of PAEs (μg/L). The dotted line refers to the NCs with no PAEs. (c, d) Selectivity of NERRA assay to PAE mixture and individual PAEs; (e, f) Selectivity of NERRA assay to PAE mixture and non-phthalate compounds (BPA and 4-NP).

band at ~245 nm decreased from 0.1711 mdeg (aptamer only) to −0.2804 mdeg (aptamer with 1 μg/L PoPo3 dye) and −0.8328 mdeg (aptamer with 5 μg/L PoPo3 dye). In general, a decrease in the intensity of the negative CD band occurs when target molecules are inserted perpendicular to the helical DNA axis [46–48]. Since the peak at ~245 nm is the only negative CD band in Fig. 3a, it is reasonable to conclude that the PoPo3 dye intercalated perpendicular to the base pairs of the aptamer.

As shown in Fig. 3b, the CD spectra suggest that the ssDNA aptamer has the typical B-form of DNA with negative and positive bands at 240 nm and 280 nm, respectively [49]. As indicated by the circle, the interaction of the PAE mixture with the ssDNA aptamer induced a CD

Table 2
P-values obtained by student's t-test to compare each sample with NC (confidence level = 99%). Note: *NC refers to PoPo3-aptamer complex in Tris-HCl buffer solution (no target).

No.	Type	Target	P-value
1	–	*NC	–
2	Phthalate	PAE Mixture	**0.000219**
3	Phthalate	PA	0.000612
4	Phthalate	DMP	0.007386
5	Phthalate	DEP	0.001798
6	Phthalate	DBP	0.002011
7	Phthalate	DIBP	0.002702
8	Phthalate	BBP	0.005440
9	Phthalate	DEHP	0.002190
10	Non-phthalate	BPA	**0.025975**
11	Non-phthalate	4-NP	**0.020818**

spectral change at ~280 nm. After the addition of the PAE mixture (1 and 10 μg/L), the positive CD band at ~280 nm decreased from 0.749 (aptamer only) to 0.391 (aptamer with 1 μg/L PAEs) and 0.414 (aptamer with 10 μg/L PAEs) $\times 10^{-3}$°, respectively. This suggests that the interaction of the PAEs with the ssDNA aptamer probably caused the conformational change of the DNA aptamer. Nonetheless, the exact binding mechanism remains to be determined. In the previous studies [35,42], a decrease in the intensity of the negative CD bands (~240 nm or 320 nm) could occur in the event of either perpendicular insertion of target molecules to the helical DNA axis or ligand transitions between the target molecule and DNA. As the change of the negative band (~240 nm) was marginal, it is unlikely that the binding is via intercalation.

3.2. Determination of suitable PoPo3 dye and ssDNA aptamer concentrations

At a given ssDNA aptamer concentration, the fluorescence ($RFU_{561\ nm}$) increased with the PoPo3 dye concentration (Fig. 3c). This is consistent with the understanding that the PoPo3 dye would be intercalated into the ssDNA aptamer, hence would increase the fluorescence. As expected, the increment in the ssDNA concentrations also resulted in the corresponding increment of the fluorescence for a given PoPo3 concentration. The plots corresponding to 0.05, 0.25, 0.5, and 2.5 μM of ssDNA aptamer are rather linear and have R^2 (coefficient of determination) values of 0.88, 0.92, 0.95, and 0.98, respectively. The regression plots are shown in Figs. S5a–S5d. The ssDNA aptamer concentration of 2.5 μM also has the best linearity (highest R^2) and exhibited the highest fluorescence over the given PoPo3 dye concentration range (0.1–10 μM). This ssDNA aptamer concentration was used throughout the subsequent experiments.

As shown in Fig. 3d, although higher PoPo3 dye concentrations corresponded to higher fluorescence values ($RFU_{561\ nm}$), they also corresponded to an observable decrease of the fluorescence over time (possibly due to photobleaching). At the highest PoPo3 dye concentration of 10 μM, the fluorescence decreased from 224.12 ± 1.70 to 197.66 ± 0.48. This is an ~11.8% decrease over a duration of 10 min. Similarly, the PoPo3 dye concentrations of 5 and 1 μM also resulted in a fluorescence decrease from 93.81 ± 6.74 to 85.00 ± 7.17 (~9.4%) and 33.33 ± 2.93 to 31.81 ± 0.95 (~4.6%), respectively. As its fluorescence decrease was less than 5% over 10 min, 1 μM was determined as a suitable PoPo3 dye concentration for the subsequent experiments.

The fluorescence values corresponding to the PoPo3 dye and ssDNA aptamer (Aptamer + PoPo3 + Buffer) concentrations of 1 and 2.5 μM, respectively, were compared to those of the two NCs (Fig. 3e). As expected, the NC (PoPo3 + Buffer) produced a lower fluorescence of 42.43 ± 0.80–47.16 ± 1.42. The other NC (Buffer) resulted in an even lower ambient measurement of 16.60 ± 2.10–20.46 ± 5.60. This is consistent with the quenching of the PoPo3 dye fluorescence in the absence of intercalation with an ssDNA aptamer.

3.3. Characterization of quantification sensitivity of NERRA assay to PAEs

The response of NERRA assay to the varying concentrations of PAE mixtures is shown in Fig. 4a. The fluorescence ($RFU_{561\ nm}$) decreased over the 30-min duration and did not appear to have reached an equilibrium. Therefore, as previously mentioned, the rate of fluorescence change $|\Delta RFU_{561}/\Delta t|$ as a cumulative representation would yield a meaningful result compared with a single-time-point measurement. For PAE mixture concentrations of 0 (NC), 0.1, 1, 5, 50, and 200 μg/L, the corresponding $|\Delta RFU_{561}/\Delta t|$ values were 0.71 ± 0.04, 1.16 ± 0.04, 1.26 ± 0.04, 1.29 ± 0.02, 1.29 ± 0.03, and 1.34 ± 0.03 (Fig. 4b). This resulted in a regression of $y = 0.048 \log(x) + 1.23$ with $R^2 = 0.71$, where y is $|\Delta RFU_{561}/\Delta t|$ and x is the PAE mixture concentration. Note that DNA based fluorescence assays (analog of the proposed NERRA assay) had calibration plots with R^2 that ranged from 0.63 to 0.94 [35,42,50,51]. And the corresponding limit of quantitation (LOQ) was 0.1 μg/L. As the environmentally relevant PAE concentrations in aquatic systems range from 0.1 to 1472 μg/L [52,53], NERRA assay is considered to have the appropriate quantification range for PAE monitoring in the environment.

3.4. Characterization of quantification selectivity of NERRA assay to PAEs

The selectivity of NERRA assay to the PAE mixture and individual PAEs is shown in Fig. 4c and Table 2. Compared to the NC, the $|\Delta RFU_{561}/\Delta t|$ value of the PAE mixture and individual PAEs showed *P*-values of less than 0.01 (student's t-test, 99% confidence level, Table 2). This indicates that their $|\Delta RFU_{561}/\Delta t|$ values are significantly different (higher) than those of the NC. In order to further appreciate the relative difference between PAE mixture and individual PAEs, the NC background $|\Delta RFU_{561}/\Delta t|$ value is first subtracted from that of all samples and then they are normalized to that of PAE mixture (Fig. 4d). It shows that the normalized $|\Delta RFU_{561}/\Delta t|$ values of PA, DMP, DEP, DBP, DIBP, BBP, and DEHP were 89%, 59%, 60%, 58%, 54%, 62% and 68% respectively. It is interesting to note that the normalized $|\Delta RFU_{561}/\Delta t|$ of PA was the highest among the PAEs. This is because PA also has the simplest structure among the phthalates (Table S1). Therefore, it is reasonable to suggest that the PA structure could be primarily responsible for the binding of the PAEs to the ssDNA aptamer.

As to the reason behind the PAE mixture yielding the highest $|\Delta RFU_{561}/\Delta t|$, it is likely due to the higher affinity of the aptamer to the PAE mixture as compared to individual PAE. For example, background subtracted normalized $|\Delta RFU_{561}/\Delta t|$ for PA only was 89%. This might suggest 11% of the aptamer did not bind to PA and might have affinity for other PAEs instead. Therefore, in a PAE mixture, an aptamer that did not bind to PA would conceivably instead bind to other PAEs. An aptamer is more likely to bind to one of the PAEs in a mixed (7 PAEs) sample as compared to a single PAE sample.

The $|\Delta RFU_{561}/\Delta t|$ of PAE mixture and other non-phthalate compounds (BPA and 4-NP) are shown in Fig. 4e. As shown in Table 2, the *P*-values of BPA and 4-NP (as compared to NC) were ~0.026 and ~0.021, while that of PAE mixture was ~0.0002. This means that the $|\Delta RFU_{561}/\Delta t|$ value of BPA and 4-NP are statistically no different from that of NC and further implies the NERRA assay has higher selectivity to PAE mixture as compared to BPA and 4-NP. In order to further appreciate the selectivity of NERRA assay to PAE mixture over BPA and 4-

Table 3
Quantitative detection of PAEs extracted from a plastic product by both NERRA assay and GC/MS analysis; the standard deviation was calculated from three measurements.

Sample information	NERRA assay, A (mg PAEs/kg sample)*	GC/MS analysis, B (mg DEHP/kg sample)	A/B × 100 (%)
Plastic Product (Picnic Mat)	164 ± 59.7	217.2 ± 10.8	75.7 ± 23.8

Note) *The majority of PAEs was identified as DEHP (Fig. S1).

NP, the background $|\Delta RFU_{561}/\Delta t|$ (which is that of NC) is subtracted from that of PAE mixture, BPA and 4-NP. They are then normalized to that of PAE mixture. As shown in Fig. 4f, the background subtracted normalized $|\Delta RFU_{561}/\Delta t|$ of BPA and 4-NP were 33% and 36%, respectively, as compared to that of PAE mixture (100%).

3.5. Quantitative detection of PAEs in the plastic product

As shown in Table 3, NERRA assay was able to quantitatively detect the PAEs in a plastic product (164 ± 59.7 mg PAEs/kg sample). Based on the GC/MS results, the peaks of which are shown in Fig. S1 with m/z ratios of 149 and 167, the predominant PAE in the plastic product was subsequently determined as DEHP (217.2 ± 10.8 mg DEHP/kg sample). This indicates that NERRA assay effectively quantified only DEHP instead of the PAE mixture. In this case, the quantification by NERRA assay was lower, 75.7 ± 23.8% of the GC/MS result. This is consistent with the earlier observation shown in Fig. 4c and d that NERRA assay quantification for DEHP only would be lower than that for the PAE mixture at a given concentration.

3.6. Quantitative detection of PAEs by custom analyzer

As expected, the output voltage (V_{out}) of the custom analyzer increased with time (t) for varying PAE mixture concentrations (Fig. 5a). More importantly, a higher PAE mixture concentration resulted in a lower V_{out}. At t = 300 s or 5 min, PAE mixture concentrations of 0, 1, 10, 50, and 100 μg/L yielded V_{out} of 2.46 ± 0.01, 1.88 ± 0.01, 1.75 ± 0.01, 1.72 ± 0.01, and 1.65 ± 0.00 V (or × 10^3 mV), respectively. The corresponding rates of output-voltage changes ($\Delta V_{out}/\Delta t$) were 7.92 ± 0.07, 6.04 ± 0.03, 5.66 ± 0.05, 5.52 ± 0.02, and 5.31 ± 0.03 mV/min, respectively (Fig. 5b and S3). Therefore, the resulting regression fit was y = - 0.34 log(x) + 6.03 (R^2 = 0.97), where y is $\Delta V_{out}/\Delta t$ and x is the PAE mixture concentration. More specifically, the PAE mixture concentration was quantified by the custom analyzer after 5 min.

Further examination of Fig. 5a would naturally lead to the possibility of a shorter time for quantification. Therefore, $\Delta V_{out}/\Delta t$ was also calculated for three more time points at t = 3, 1, and 0.5 min (30 s). The results are shown in Fig. 5c, d, and 5e, respectively, as well as in Fig. S3. Particularly at t = 30 s, the PAE mixture concentrations of 0, 1, 10, 50, and 100 μg/L yielded V_{out} values of 8.45 ± 0.12, 6.50 ± 0.02, 6.03 ± 0.04, 5.94 ± 0.01, and 5.69 ± 0.04 mV/min, respectively. This also provided a similar regression line of y = - 0.37 log(x) + 6.47 (R^2 = 0.94). Thus, the custom analyzer was able to perform the quantitative detection of PAEs in as quickly as 30 s with an LOQ of 1 μg/L.

3.7. Potential and limitations of NERRA assay

Using a commercial spectrofluorometer, NERRA assay was able to quantitatively detect a PAE mixture in 30 min with an LOQ of 0.1 μg/L. Using the portable custom analyzer, the detection time was shortened to 30 s with a tradeoff in the LOQ (1 μg/L). In both cases, the LOQs remain within the environmentally relevant PAE concentrations of 0.1–1472 μg/L. Given the small footprint of the custom analyzer, as shown in Fig. 2, the portability of NERRA assay is evident. Table 1 shows another optical fiber-based detection immunoassay for a PAE mixture by Tang et al. [28]. It has an LOQ of 0.01 μg/L but required 40 min to obtain results. This assay also did not demonstrate assay selectivity as well as portability. As mentioned earlier, it is unsurprising that the sensitivity of NERRA assay to a specific PAE (such as DEHP, DIBP, or DBP) is lower than that by other DEHP-specific methods, such as by Han et al. [34], and Lim et al. [35]. However, similar to other single-PAE detection methods [29–37], their detection times varied from 30 min to 21 h. In addition, all of these methods (other than Lim et al., 2018) did not demonstrate a portability. For Lim et al., 2018, the portability was demonstrated but its LOQ was not reported [35].

4. Conclusion

We have demonstrated a non-equilibrium rapid replacement aptamer (NERRA) assay that could perform ultra-fast quantitative detection of a PAE mixture (PA, DMP, DEP, DBP, DIBP, BBP, and DEHP) without waiting for the reaction to reach equilibrium. Using PoPo3 dye (1 μM) intercalated into an ssDNA aptamer (2.5 μM), the PAE mixture concentration could be measured in 30 min via a commercial spectrofluorometer with a corresponding LOQ of 0.1 μg/L. The selectivity of NERRA assay to PAEs over non-phthalate compounds, such as BPA and 4-NP, was also demonstrated. Furthermore, NERRA assay was able to quantitatively detect 164 ± 59.7 mg PAEs/kg sample (mostly DEHP) in a plastic product (picnic mat). The result was less than that via GC/MS at 217.2 ± 10.8 mg DEHP/kg sample and consistent with the understanding that NERRA assay is less sensitive to individual PAEs. Instead of using a commercial spectrofluorometer, NERRA assay could also be operated via a custom analyzer. This significantly reduces the detection time to 30 s with a tradeoff of the LOQ (1 μg/L). More specifically, the NERRA assay via the portable custom analyzer could perform ultra-fast (30 s) quantitative detection of PAEs that were at environmentally relevant concentrations.

Author statement

Dabin Kim performed experiments, analyzed data, and drafted manuscript Hyun Jeong Lim performed experiments and analyzed data (DNA intercalation). Yun Gyong Ahn performed experiments and analyzed data (GC/MS analysis). Beelee Chua designed device, developed overall measurement scheme, revised manuscript, and provided engineering oversight. Ahjeong Son designed biosensor, analyzed data, revised manuscript, and provided scientific oversight.

Declaration of competing interest

The authors declare that they have no known competing financial interests or personal relationships that could have appeared to influence the work reported in this paper.

Acknowledgements

This work was supported by the National Research Foundation of Korea (NRF-2019R1A2C2 084233, NRF-2019R1F1A1 058562). The authors appreciate the experimental assistance from Seo Won Cho, Ki

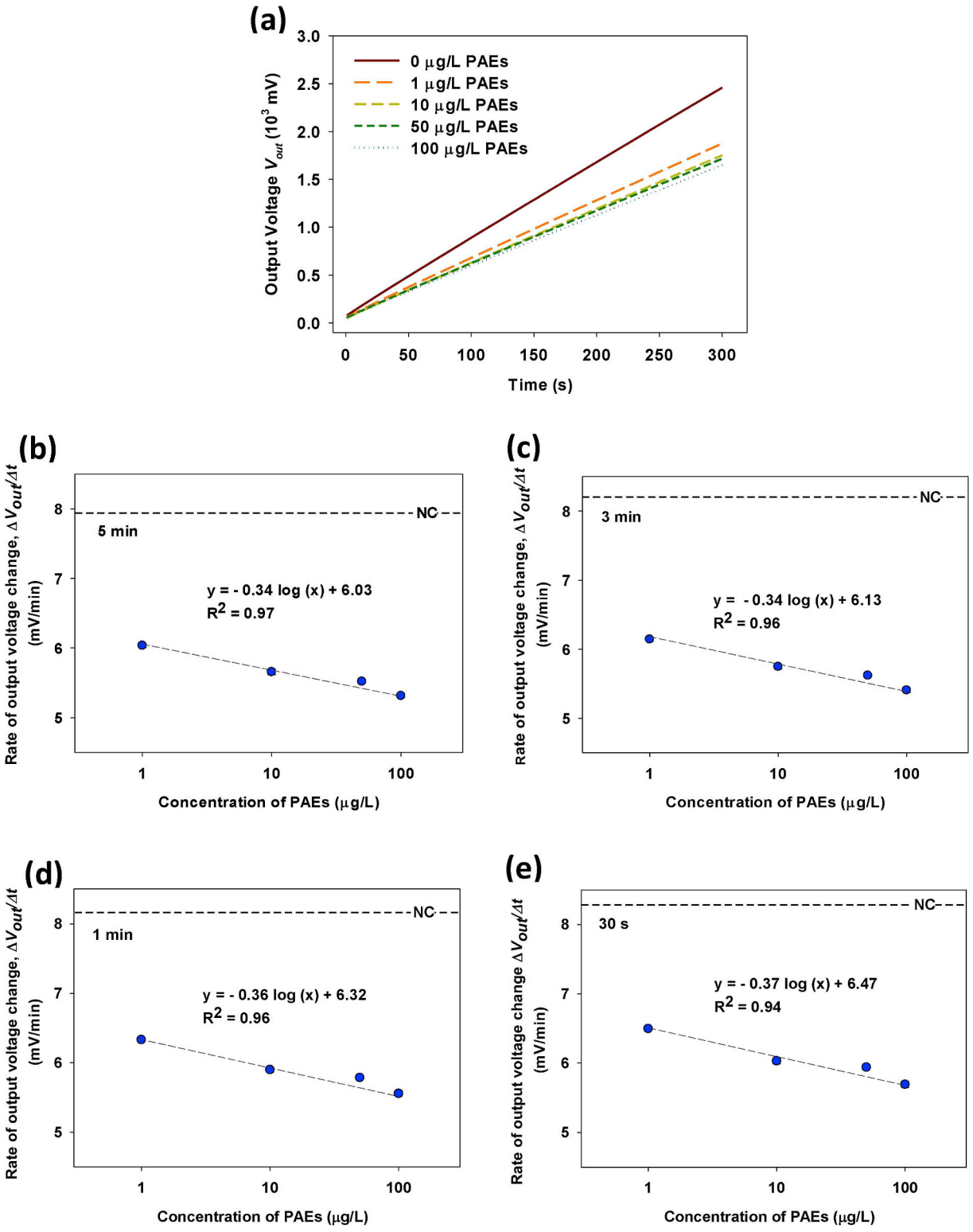

Fig. 5. (a) Output voltage V_{out} (10^3 mV) versus time (s) for varying PAE concentrations; Rate of output voltage change $\Delta V_{out}/\Delta t$ (mV/min) versus concentration of PAEs (μg/L) at (b) 5 min, (c) 3 min, (d) 1 min, and (e) 30 s.

Ae Kim, and Minkyung Kang. The authors also acknowledge Prof. Ji Yi Lee for her support for the GC/MS analysis.

Appendix A. Supplementary data

Supplementary data to this article can be found online at https://doi.org/10.1016/j.talanta.2020.121216.

References

[1] P.F. Bruins, Plasticizer Technology, Reinhold Publishing, New York, 1965.
[2] A.S. Wilson, Plasticizers: Principles and Practice, Institute of Materials, London, 1995.
[3] G. Matthews, PVC: Production, Properties and Uses, The Institute of Materials, London, 1996.
[4] Q. Yu, A.P.S. Selvadurai, Mechanical behaviour of a plasticized PVC subjected to

ethanol exposure, Polym. Degrad. Stabil. 89 (2005) 109–124.
[5] C.E. Mackintosh, J.A. Maldonado, M.G. Ikonomou, F.A.P.C. Gobas, Sorption of phthalate esters and PCBs in a Marine ecosystem, Environ. Sci. Technol. 40 (2006) 3481–3488.
[6] Z. Xie, R. Ebinghaus, C. Temme, R. Lohmann, A. Caba, W. Ruck, Occurrence and air-sea exchange of phthalates in the Arctic, Environ. Sci. Technol. 41 (2007) 4555–4560.
[7] T. Schettler, Human exposure to phthalates via consumer products, Int. J. Androl. 29 (2006) 134–139.
[8] R. Benson, Hazard to the developing male reproductive system from cumulative exposure to phthalate esters-dibutyl phthalate, diisobutyl phthalate, butylbenzyl phthalate, diethylhexyl phthalate, dipentyl phthalate, and diisononyl phthalate, Regul. Toxicol. Pharmacol. 53 (2009) 90–101.
[9] A. Guart, F. Bono-Blay, A. Borrell, S. Lacorte, Migration of plasticizerphthalates, bisphenol A and alkylphenols from plastic containers and evaluation of risk, Food Addit. Contam. 28 (2011) 676–685.
[10] D. Koniecki, R. Wang, R.P. Moody, J. Zhu, Phthalates in cosmetic and personal care products: concentrations and possible dermal exposure, Environ. Res. 111 (2011) 329–336.
[11] A.O. Earls, I.P. Axford, J.H. Braybrook, Gas chromatography-mass spectrometry determination of the migration of phthalate plasticisers from polyvinyl chloride toys and childcare articles, J. Chromatogr. A 983 (2003) 237–246.
[12] J.A. Tickner, T. Schettler, T. Guidotti, M. McCally, M. Rossi, Health risks posed by use of di-2-ethylhexyl phthalate (DEHP) in PVC medical devices: a critical review, Am. J. Ind. Med. 39 (2001) 100–111.
[13] P. Ventrice, D. Ventrice, E. Russo, G.D. Sarro, Phthalates: european regulation, chemistry, pharmacokinetic and related toxicity, Environ. Toxicol. Pharmacol. 36 (2013) 88–96.
[14] K. Becker, M. Seiwert, J. Angerer, W. Heger, H.M. Koch, R. Nagorka, E. Roßkamp, C. Schlüter, B. Seifert, D. Ullrich, DEHP metabolites in urine of children and DEHP in house dust, Int. J. Hyg Environ. Health 207 (2004) 409–417.
[15] J.C. Caldwell, DEHP: genotoxicity and potential carcinogenic mechanisms, Mutat. Res. Rev. Mutat. Res. 751 (2012) 82–157.
[16] K.J. Johnson, N.E. Heger, K. Boekelheide, Of mice and men (and rats): phthalate-induced fetal testis endocrine disruption is species-dependent, Toxicol. Sci. 129 (2012) 235–248.
[17] S. Heise, N. Litz, German Phthalates, Federal Environmental Agency, Berlin. Germany, 2004, pp. 1–41.
[18] Epa, Edition of the Drinking Water Standards and Health Advisories, U.S. Environmental Protection Agency, Washington DC, U.S., 2006, pp. 1–18 2006.
[19] J. Boberg, S. Metzdorff, R. Wortziger, M. Axelstad, L. Brokken, A.M. Vinggaard, M. Dalgaard, C. Nellemann, Impact of diisobutyl phthalate and other PPAR agonists on steroidogenesis and plasma insulin and leptin levels in fetal rats, Toxicology 250 (2008) 75–81.
[20] R. Mankidy, S. Wiseman, H. Ma, J.P. Giesy, Biological impact of phthalates, Toxicol. Lett. 217 (2013) 50–58.
[21] S.H. Swan, Environmental phthalate exposure in relation to reproductive outcomes and other health endpoints in humans, Environ. Res. 108 (2008) 177–184.
[22] Y. Wang, G. Zhang, L. Wang, Potential toxicity of phthalic acid esters plasticizer: interaction of dimethyl phthalate with trypsin in vitro, J. Agric. Food Chem. 63 (2014) 75–84.
[23] EU Commission regulation (EU), 2018/2005 of 17 December 2018 Amending Annex XVII to Regulation (EC) No 1907/2006 of the European Parliament and of the Council Concerning the Registration, Evaluation, Authorisation and Restriction of Chemicals (REACH) as Regards Bis(2-Ethylhexyl) Phthalate (DEHP), Dibutyl Phthalate (DBP), Benzyl Butyl Phthalate (BBP) and Diisobutyl Phthalate (DIBP), off. J. Eur. Union, Finland, Helsinki, 2018, pp. 1–6.
[24] H.-Y. Shen, H.-L. Jiang, H.-L. Mao, G. Pan, L. Zhou, Y.-F. Cao, Simultaneous determination of seven phthalates and four parabens in cosmetic products using HPLC-DAD and GC-MS methods, J. Separ. Sci. 30 (2007) 48–54.
[25] J. Li, Y. Cai, Y. Shi, S. Mou, G. Jiang, Analysis of phthalates via HPLC-UV in environmental water samples after concentration by solid-phase extraction using ionic liquid mixed hemimicelles, Talanta 74 (2008) 498–504.
[26] Y.-L. Feng, X. Liao, G. Grenier, N. Nguyen, P. Chan, Determination of 18 phthalate metabolites in human urine using a liquid chromatography-tandem mass spectrometer equipped with a core-shell column for rapid separation, Anal. Methods 7 (2015) 8048–8059.
[27] M. Chen, L. Tao, E.M. Collins, C. Austin, C. Lu, Simultaneous determination of multiple phthalate metabolites and bisphenol-A in human urine by liquid chromatography-tandem mass spectrometry, J. Chromatogr. B Analyt. Technol. Biomed. Life Sci. 904 (2013) 73–80.
[28] M. Tang, Y. Wu, D. Deng, J. Wei, J. Zhang, D. Yang, G. Li, Development of an optical fiber immunosensor for the rapid and sensitive detection of phthalate esters, Sensor. Actuator. B Chem. 258 (2018) 304–312.
[29] M. Zhang, W. Hong, X. Wu, Y. Zhang, F. Li, S.-Q. Zhao, A highly sensitive and direct competitive enzyme-linked immunosorbent assay for the detection of di-(2-ethylhexyl) phthalate (DEHP) infant supplies, Anal. Methods 7 (2015) 5441–5446.
[30] X. Cui, P. Wu, D. Lai, S. Zheng, Y. Chen, S.A. Eremin, W. Peng, S. Zhao, Development of a highly specific fluorescence immunoassay for detection of diisobutyl phthalate in edible oil samples, J. Agric. Food Chem. 63 (2015) 9372–9378.
[31] M.-C. Zhang, Q.-E. Wang, H.-S. Zhuang, Determination of dibutyl o-phthalate by antigen-coated competitive fluorescence immunoassay, Anal. Lett. 40 (2007) 127–137.
[32] H. Kuang, L. Xu, G. Cui, W. Ma, C. Xu, Development of determination of di-n-octyl phthalate (DOP) residue by an indirect enzyme-linked immunosorbent assay, Food Agric. Immunol. 21 (2010) 265–277.
[33] H. Kuang, L. Liu, L. Xu, W. Ma, L. Guo, L. Wang, C. Xu, Development of an enzyme-linked immunosorbent assay for dibutyl phthalate in liquor, Sensors 13 (2013) 8331–8339.
[34] Y. Han, D. Diao, Z. Lu, X. Li, Q. Guo, Y. Huo, Q. Xu, Y. Li, S. Cao, J. Wang, Y. Wang, J. Zhao, Z. Li, M. He, Z. Luo, X. Lou, Selection of group-specific phthalic acid esters binding DNA aptamers via rationally designed target immobilization and applications for ultrasensitive and highly selective detection of phthalic acid esters, Anal. Chem. 89 (2017) 5270–5277.
[35] H.J. Lim, A.-R. Kim, M.-Y. Yoon, Y. You, B. Chua, A. Son, Development of quantum dot aptasensor and its portable analyzer for the detection of di-2-ethylhexyl phthalate, Biosens. Bioelectron. 121 (2018) 1–9.
[36] W. Xu, T. Li, W. Huang, Y. Luan, Y. Yang, S. Li, W. Yang, A magnetic fluorescence molecularly imprinted polymer sensor with selectivity for dibutyl phthalate via Mn doped ZnS quantum dots, RSC Adv. 7 (2017) 51632–51639.
[37] S. Xiong, J. Cheng, L. He, M. Wang, X. Zhang, Z. Wu, Detection of di(2-ethylhexyl) phthalate through graphene–β-cyclodextrin composites by electrochemical impedance spectroscopy, Anal. Methods 6 (2014) 1736–1742.
[38] M. McKeague, R. Velu, K. Hill, V. Bardoczy, T. Meszaros, M.C. DeRosa, Selection and characterization of a novel DNA aptamer for label-free fluorescence biosensing of ochratoxin A, Toxins 6 (2014) 2435–2452.
[39] L. Kong, J. Xu, Y. Xu, Y. Xiang, R. Yuan, Y. Chai, A universal and label-free aptasensor for flurorescent detection of ATP and thrombin based on SYBR Green I dye, Biosens. Bioelectron. 42 (2013) 193–197.
[40] Y. Xu, J. Xu, Y. Xiang, R. Yuan, Y. Chai, Target-induced structure switching of hairpin aptamers for label-free and sensitive fluorescent detection of APT via exonuclease-catalyzed target recycling amplification, Biosens. Bioelectron. 51 (2014) 293–296.
[41] Y. Tan, X. Zhang, Y. Xie, R. Zhao, C. Tan, Y. Jiang, Label-free fluorescent assays based on aptamer-target recognition, Analyst 137 (2012) 2309–2312.
[42] E.-H. Lee, A. Son, Fluorescence resonance energy transfer based quantum dot-Aptasensor for the selective detection of microcystin-LR in eutrophic water, Chem. Eng. J. 359 (2019) 1493–1501.
[43] H. Zhang, D. Zhou, A quantum dot-intercalating dye dual-donor FRET based biosensor, Chem. Commun. 48 (2012) 5097–5099.
[44] C.-W. Chi, Y.-H. Lao, Y.-S. Li, L.-C. Chen, A quantum dot-aptamer beacon using a DNA intercalating dye as the FRET reporter: application to label-free thrombin detection, Biosens. Bioelectron. 26 (2011) 3346–3352.
[45] B. Tienpont, F. David, E. Dewulf, P. Sandra, Pitfalls and solutions for the trace determination of phthalates in water samples, Chromatographia 61 (2005) 365–370.
[46] C.A. Frederick, L.D. Williams, G. Ughetto, G.A. van der Marel, J.H. van Boom, A. Rich, A.H. Wang, Structural comparison of anticancer drug-DNA complexes: adriamycin and daunomycin, Biochemistry 29 (1990) 2538–2549.
[47] N. Berova, P.I. Polavarapu, K. Nakanishi, R.W. Woody, Comprehensive Chiroptical Spectroscopy: Applications in Sterochemical Analysis of Synthetic Compounds, Natural Products, and Biomolecules, Wiley2012.
[48] M. Deiana, B. Mettra, K. Matczyszyn, K. Piela, D. Pitrat, J. Olesiak-Banska, C. Moonereau, C. Andraud, M. Samoc, Interactions of a biocompatible water-soluble anthracenyl polymer derivative with double-stranded DNA, Phys. Chem. Chem. Phys. 17 (2015) 30318–30327.
[49] J. Kypr, I. Kejnovská, D. Renčiuk, M. Vorlíčková, Circular dichroism and conformational polymorphism of DNA, Nucleic Acids Res. 37 (2009) 1713–1725.
[50] H.J. Lim, B. Chua, A. Son, Detection of bisphenol A using palm-size NanoAptamer analyzer, Biosens. Bioelectron. 94 (2017) 10–18.
[51] E.-H. Lee, K.-S. Cho, A. Son, Detection and quantification of toxin-producing *Microcystis aeruginosa* strain in water by NanoGene assay, J. Microbiol. Biotechnol. 27 (2017) 808–815.
[52] H. Fromme, T. Küchler, T. Otto, K. Pilz, J. Müller, A. Wenzel, Occurrence of phthalates and bisphenol A and F in the environment, Water Res. 36 (2002) 1429–1438.
[53] W.J.G.M. Peijnenburg, J. Struijs, Occurrence of phthalate esters in the environment of The Netherlands, Ecotox, Environ. Safe. 63 (2006) 204–215.